



ELSEVIER

Biophysical Chemistry 105 (2003) 67–77

Biophysical
Chemistry

www.elsevier.com/locate/bpc

The pH dependence of HIV-1 capsid assembly and its interaction with cyclophilin A

Marjorie BonHomme^a, Stanislaus Wong^b, Carol Carter^c, Suzanne Scarlata^{a,*}

^a*Department of Physiology and Biophysics, State University of New York at Stony Brook, Stony Brook, NY 11794, USA*

^b*Department of Chemistry, State University of New York at Stony Brook, Stony Brook, NY 11794, USA*

^c*Department of Microbiology, State University of New York at Stony Brook, Stony Brook, NY 11794, USA*

Received 19 February 2003; received in revised form 26 March 2003; accepted 26 March 2003

Abstract

Immature HIV-1 virions have spherical cores which become conical due to cleavage of the capsid domain of Gag. Here, we have used an immature form of capsid and show by electron microscopy, atomic force microscopy and single angle light scattering that it aggregates to spherical cores resembling immature virions at high ionic strengths and at pH values above 6. Dynamic angle light scattering of the dissociated protein shows structural changes that promote oligomerization above pH 6. We then examined the role of the required host protein cyclophilin A on assembly. Cyclophilin A is incorporated into virions at a 1:10 cyclophilin A/capsid ratio. We find that although cyclophilin A does not affect the oligomerization rate or stability of immature capsid cores, it does bind strongly to immature capsid at physiological stoichiometry above pH 6. This association serves as an entry route of cyclophilin A into HIV-1 virions.

© 2003 Elsevier B.V. All rights reserved.

Keywords: HIV assembly; HIV capsid; Cyclophilin A; Fluorescence; Atomic force microscopy; Dynamic light scattering

1. Introduction

Human immunodeficiency virus (HIV) is a member of the *Retroviridae* family (for background information see Coffin et al. [1]). A central theme in retroviral assembly is the coordinated use of large precursor polyproteins like Gag. Approximately 1500–2500 copies of Gag self-associate and bind two unspliced copies of RNA before binding to the cell membrane via the matrix

domain of Gag. The virus buds from the host cell and then undergoes maturation, which is characterized by a morphological transition from a spherical to a conical-shaped core to give an infectious particle. During subsequent infection, the core disassembles in the cytosol of the newly infected host cell. Disassembly releases a reverse transcription/preintegration complex that is responsible for the synthesis of proviral DNA and its subsequent nuclear localization and chromosomal integration.

During maturation, Gag is proteolytically cleaved by the viral protease into three major structural proteins: matrix, capsid, and nucleocap-

*Corresponding author. Tel.: +1-631-444-3071; fax: +1-631-444-3432.

E-mail address: suzanne.scarlata@sunysb.edu (S. Scarlata).

sid [1]. Matrix initially targets Gag to the plasma membrane and remains membrane-bound in the virion. However, some of it may dissociate from the membrane upon entry into the host cell to become part of the preintegration complex [2–4]. The capsid forms the conical core that encapsulates the RNA–protein complex and disassembles upon entry of the virus into host cells. Nucleocapsid binds specifically to viral RNA forming a ribonucleoprotein complex.

HIV type 1 (HIV-1) requires the cytosolic protein cyclophilin A (CypA) from host cells for infectivity [5]. CypA is a peptidyl-prolyl *cis-trans* isomerase [6] and has chaperone activity in cells [7]. CypA is specifically incorporated into HIV-1 virions via its interaction with the capsid domain of Gag [8–10]. Using radiolabeling, gel densitometry and immunoblot analysis it was shown that for every 10 Gag molecules, 1 CypA molecule is incorporated into the virion [8,9,11]. The CypA binding site on HIV-1 capsid is localized to a proline-rich flexible exposed loop that lies in the amino terminal domain [8,9,12–14] and includes residues 85–93 [12,14,15], which encompasses the critical residue Pro90 [8,12,13,16]. Disruption of the cyclophilin A/capsid interaction by either cyclosporin [8–10], its analogs [17,18], mutagenesis of residues in the binding site [19–22] or deletion of the CypA gene [23] blocks CypA incorporation into virions and greatly reduces HIV-1 viral replication and therefore infectivity. Removal of cellular CypA has no visible effect on virus assembly, budding or maturation [24].

Capsid (CA) gives the HIV virus its distinctive conical structure in contrast to the typical spherical form seen in immature HIV virions and other retroviruses. In this study, we used aminohexahistidine tagged-CA (N His6-CA) as a model for immature capsid. In the Gag precursor, the amino terminus of capsid is linked to the matrix domain. Recent NMR studies of matrix protein linked to the N-terminal region of capsid shows that cleavage of matrix liberates Pro1 of capsid to form a salt bridge with Asp51 connected by a β hairpin turn [25]. This β -hairpin turn appears to adversely affect the CypA binding site which may promote dissociation of the complex as the virus matures [25].

In this study, we have used a capsid with a hexahistidine tag attached to the N-terminus in order to prevent the formation of the Pro1–Asp51 salt bridge and thus allow us to study an immature form of the capsid. The amino terminal extension on the HIV-1 capsid results in a protein that can assemble *in vitro* into hollow spheres resembling the shape of an immature virion [26,27]. Removal of the amino terminal extension from the capsid, which can be paralleled to viral maturation by proteolysis of Gag, results in the formation of cylindrical particles [27–29]. *In vitro* formation of cores using an amino terminally-extended capsid requires high protein concentration and high ionic strength [26].

The physiological basis for the need of high ionic strengths to form immature viral cores may stem from the need to assemble highly charged species. Before budding at the plasma membrane of the host cell, Gag molecules assemble on viral RNA via the zinc fingers of nucleocapsid [30,31]. Assembly of Gag on RNA results in reduction of dimensionality, which has the effect of locally increasing Gag concentration and promoting Gag assembly. The presence of negatively charged lipids, basic residues on the matrix and nucleocapsid domains of Gag, and negatively charged RNA all work to increase local electrostatic conditions and may promote assembly of the whole virus.

Although lipid membranes and RNA are clearly needed for HIV-1 Gag assembly, our previous work has shown that the capsid must make critical contacts in order for assembly to proceed [32]. The observations that the capsid itself can form structures that mimic the mature and immature forms, as discussed above, support this idea. Here, we have used an immature form of capsid to study environmental factors that promote assembly. We find that as the pH is raised to values above 6.0, capsid monomers undergo condensation to an ‘oligomerization-ready’ form. Not only does this form have a high potential to self-associate, but it is also able to form strong, specific contacts with CypA. These contacts with CypA do not affect assembly, but rather serve to promote CypA insertion into the virion at the specific, physiological stoichiometry.

2. Materials and methods

2.1. Constructs

The HIV-1 capsid sequence was derived from pBH10, GenBank Accession Number M15654 [33]. To simplify purification, the CA sequence was subcloned into pB6, a derivative of pET 11d (Novagen, Madison, WI, USA) that expresses aminohexahistidine tagged-proteins. The entire insert region was confirmed by DNA sequencing. Glutathione *S*-transferase (GST) cyclophilin A was a gift from Braaten and Luban [19], Department of Microbiology, College of Physicians and Surgeons of Columbia University.

2.2. Recombinant protein expression and purification

N His6-CA protein was expressed in *Escherichia coli* (*E. coli*) strain BL21 (DE3) and purified by gravity chromatography using Ni-NTA Superflow resin under native conditions as described by the manufacturer (Qiagen). Successive washing with 250 mM imidazole eluted bound N His6-CA and N His6-CA was found to be >95% pure by sodium dodecyl sulfate-polyacrylamide gel electrophoresis and Coomassie staining. N His6-CA was dialyzed into 30 mM MES pH 6, 1 mM EDTA, 1 mM DTT and 20% glycerol and stored at -70°C .

GST-cyclophilin A protein was expressed in *E. coli* strain c600 and purified by gravity chromatography using glutathione sepharose resin under native conditions as described by the manufacturer (Amersham Biosciences, Piscataway, NJ, USA). The GST moiety was cleaved off using the endoprotease, thrombin. Cyclophilin A was found to be >95% pure by sodium dodecyl sulfate-polyacrylamide gel electrophoresis and coomassie staining. Cyclophilin A was dialyzed into 50 mM Tris pH 8, 30 mM NaCl and 0.5 mM DTT. After dialysis, sodium azide (0.004%) was added to cyclophilin A and cyclophilin A was stored at 4°C . Protein concentrations were determined using Bio-Rad Protein Assay Dye Reagent Concentrate (Bio-Rad Laboratories, Hercules, CA, USA).

2.3. Extent of N His6-CA oligomerization under different pHs

N His6-CA (~ 4.6 mg/ml) was dialyzed into 100 mM NaH_2PO_4 and 1 M NaCl at pHs 6, 7 and 8 overnight followed by dilution to 1.6 mg/ml. Single angle light scatter measurements were made on an ISS[®] PC1[™] photon counting spectrofluorometer (I.S.S., Inc, Champaign, IL, USA) in 3-mm quartz cuvettes at an angle 90° of the incident light (340 nm). Buffer measurements were subtracted from sample measurements.

2.4. Atomic force microscopy

Aliquots (~ 5 μl) of the capsid solution in aqueous buffer were allowed to adsorb onto freshly cleaved mica for 0.5–1 min prior to spin-drying. The samples were then subsequently rinsed with buffer and deionized, distilled water (10–50 μl) to remove loosely bound protein and buffer salts, and spun dry each time. All images on the adsorbed protein were carried out with etched Si ($k=1-5$ N/m, Digital Instruments, Santa Barbara, CA, USA) tips under ambient conditions with a Nanoscope IIIa Multimode scanning probe instrument (Digital Instruments, Santa Barbara, CA, USA) operated in TappingMode[™]. Scanning parameters varied with individual tips and samples. However, typical ranges were as follows. Drive amplitude and setpoint parameters were adjusted to apply a force sufficient to ensure ‘light’ tapping for both types of tips. The scan rates used varied from 0.5 to 2 Hz, while resonant frequencies were in the 60–80 kHz range with oscillation amplitudes of 15–75 nm. Image analysis was performed using Excel on the digitized images.

2.5. Labeling N His6-CA with acrylodan

Capsid contains two Cys residues which were modified at a 1:1 stoichiometric ratio with the probe acrylodan (6-acryloyl-2-dimethylaminonaphthalene). Acrylodan was purchased from Molecular Probes, Inc. (Molecular Probes, Inc., Eugene, OR, USA). N His6-CA (0.13 μmoles) was incubated with acrylodan (0.5 μmoles) in 100 mM NaH_2PO_4 pH 8 for 2 h at room temperature on a

rotary shaker. Unreacted acrylodan was removed using P-2 size exclusion gel (Bio-Rad Laboratories, Hercules, CA, USA) and 100 mM NaH_2PO_4 , pH 7 as the eluent. Typically 40–80% of capsid molecules were labeled with a single acrylodan molecule. Protein concentration was determined using Bio-Rad Protein Assay Dye Reagent Concentrate (Bio-Rad Laboratories, Hercules, CA, USA). The extent of labeling was estimated using the following formula:

$$\frac{A_x}{\varepsilon} \times \frac{\text{MW of capsid}}{\text{mg capsid/ml}} = \frac{\text{moles of acrylodan}}{\text{moles of capsid}}$$

where A_x is the absorbance value of acrylodan at its absorption maximum (390 nm) and ε is the molar extinction coefficient of acrylodan ($20\,000\text{ cm}^{-1}\text{ M}^{-1}$) at 390 nm.

2.6. Binding affinities as measured by fluorescence spectroscopy

All fluorescent measurements were made using an ISS[®] PC1[™] photon counting spectrofluorometer (I.S.S. Inc, Champaign, IL, USA) and quartz microcuvettes with a path length of 3 mm. Excitation wavelength was set to 380 nm while the emission wavelength was scanned from 400 to 600 nm. Acrylodan-labeled N His6-CA (2 μM) in 100 mM NaH_2PO_4 at pH 6, 7 and 8, was titrated with cyclophilin A (3 μM). Binding was measured by using the spectral area of the emission spectra (see Section 2.10).

2.7. Core formation

N His6-CA (18 mg) was dialyzed overnight into 50 mM Tris pH 8 and 1 M NaCl. To form cores, N His6-CA was incubated at 37 °C for 1 h [26]. Protein concentration was determined using Bio-Rad Protein Assay Dye Reagent Concentrate (Bio-Rad, Hercules, CA, USA).

2.8. Rate of core formation

Measurements were made on an ISS[®] PC1[™] photon counting spectrofluorometer (I.S.S. Inc., Champaign, IL, USA) in 10-mm quartz cuvettes

with constant stirring. N His6-CA (1.6 mg/ml) in 50 mM Tris pH 8 and 1 M NaCl was incubated at 37 °C while its oligomerization state was monitored using single angle light scatter with an incident light of 340 nm set at a 90° scattering angle. This was repeated in the presence of cyclophilin A (0.13 mg/ml) at the physiologically relevant ratio of 1 cyclophilin A for every 10 capsid molecules.

2.9. Pressure dissociation of cores as monitor by single angle light scatter

Cores made of N His6-CA protein (1.6 mg/ml), formed either in the presence or absence of cyclophilin A (0.13 mg), were loaded into a silanized, bottle shaped quartz cuvette topped with a polyethylene lid for transmission of pressure. The cuvette was placed into a high-pressure cell made of heat-treated Vascomax, which was connected to a pressure generator (High Pressure Equipment Company, Erie, PA, USA) through a high-pressure line also made of Vascomax. Pressure was generated through the compression of 100% ethanol. The windows of the cell are made of sapphire and are set 90 °C from each other to allow light measurement. Single angle light scattering measurements were collected at an angle 90° of the incident light (340 nm). The pressure was increased in steps of 250 bars allowing 5 min for equilibrium to be reached. Single angle light scatter measurements were made on an ISS[®] PC1[™] photon counting spectrofluorometer (ISS[®] Inc., Champaign, IL, USA)

2.10. Data analysis

To measure binding affinities, the resulting acrylodan-labeled N His6-CA emission spectra was integrated from 400 to 600 nm. Control studies substituted buffer for cyclophilin A. Changes are reported based on changes in the normalized spectral area:

Normalized spectral area

$$= \frac{\left(\sum_{\lambda=400\text{ nm}}^{\lambda=600\text{ nm}} I \right)_x - \left(\sum_{\lambda=400\text{ nm}}^{\lambda=600\text{ nm}} I \right)_i}{\left(\sum_{\lambda=400\text{ nm}}^{\lambda=600\text{ nm}} I \right)_f}$$

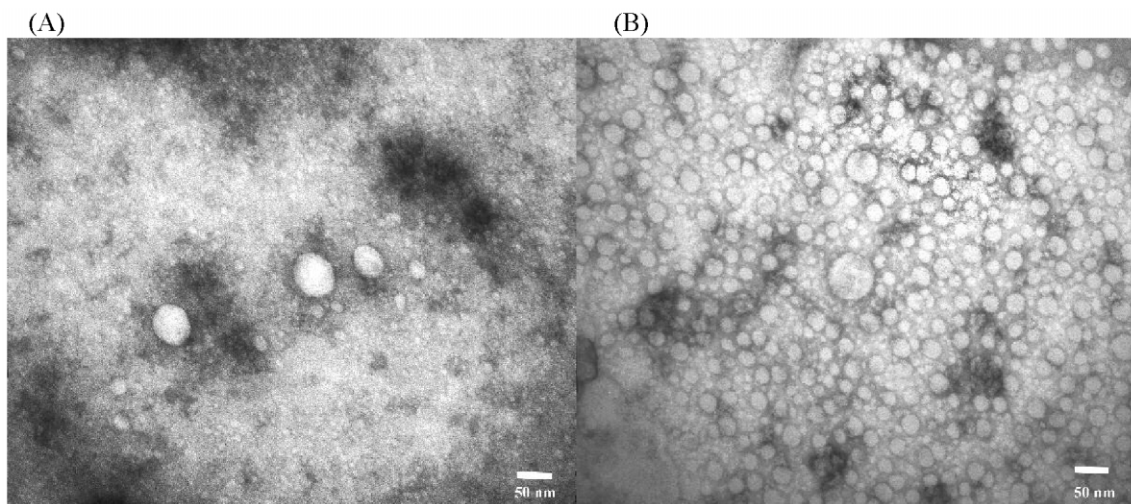


Fig. 1. Negative-stain electron micrograph of in vitro assembly products. N His6-CA (113 μ M) were dialyzed overnight against 100 mM NaH_2PO_4 , either pH 6 (panel A) or pH 8 (panel B), and 1 M NaCl and incubated at 37 $^\circ\text{C}$. The samples were stained with 1% uranyl acetate.

where I is intensity, and i is initial, x is intermediate and f is final concentration of cyclophilin A.

3. Results

3.1. N His6-CA forms cores more efficiently at pH 8 and 7 as opposed to pH 6 in the presence of 1 M NaCl

Using single angle and dynamic light scattering techniques, our laboratories have previously shown that at pH 6 and high ionic strengths (i.e. 1 M) purified mature capsid is largely monomeric, whereas raising the pH to 8 resulted in the formation of higher order capsid aggregates [34]. To test whether this pH-dependent aggregation would occur for N His6-CA, which is our model for immature capsid, we characterized the structures using electron microscopy. Protein samples at 113 μ M were prepared in 100 mM phosphate buffer at either pH 6.0 or pH 8.0 and 1 M NaCl. The results are shown in Fig. 1A,B. At pH 8 we find dense, uniform spheres similar to the immature cores structures [35,36], whereas at pH 6 we only find a small amount of disperse aggregates.

The structures seen by EM were further characterized by atomic force microscopy (AFM).

Again, samples were prepared by dialyzing purified N His6-CA into 100 mM NaH_2PO_4 , 1 M NaCl at pH 6 and 8, depositing a layer of protein on mica by spinning and then drying, and then imaged. We note that under these conditions the samples may have undergone some flattening.

In Fig. 2a,b we show the resulting AFM images. At pH 6 we find disperse spherical structures indicating a network of capsid monomers whose units corresponded to the size of the protein (3.5×7 nm) [37]. Aggregates at this pH were scarce (~ 5 in a $1 \mu\text{m}^2$ area) with heights and diameters corresponding to capsid tetramers and octomers. In contrast, at pH 8, capsid oligomers were observed at a three-fold higher density and began to aggregate into larger structures.

Taken together, the images in Figs. 1 and 2 show that the formation of spherical core structures by immature capsid is a pH-dependent process and that aggregation will be promoted above pH 6. We also note that the pH-dependent aggregation of N His6-CA seen here is comparable to that observed by dynamic light scattering for a mature capsid [34].

To relate the above images to the behavior of immature capsid in solution, we carried out a series of single angle light scatter experiments as

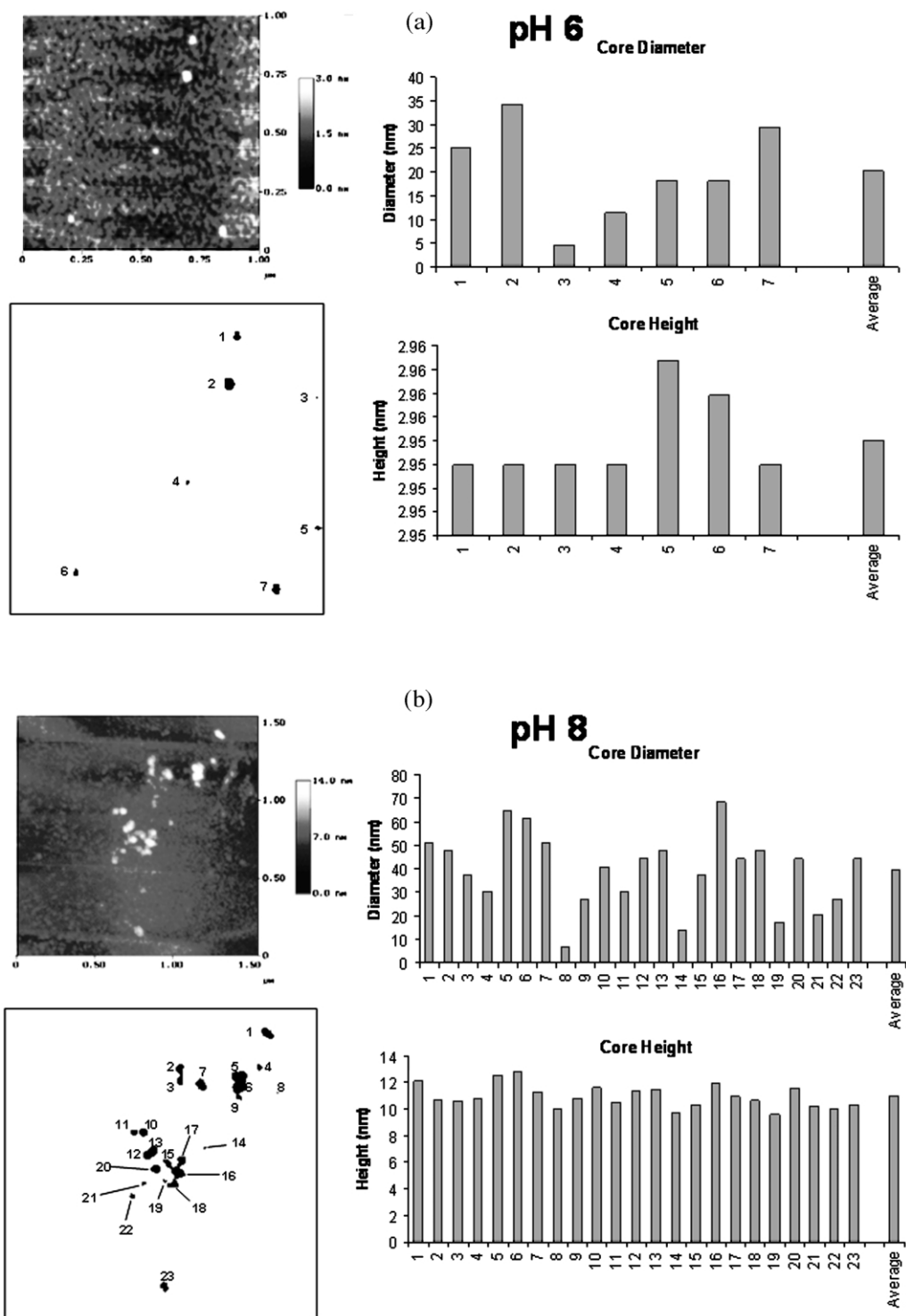


Fig. 2. Atomic force microscopy images of *in vitro* assembly products. Panel (a) shows N His6-CA (113 μ M) aggregates at pH 6 in 100 mM NaH_2PO_4 and 1 M NaCl followed by 1 h incubation at 37 $^\circ\text{C}$. Panel (b) shows N His6-CA aggregates at pH 8. All other conditions were the same.

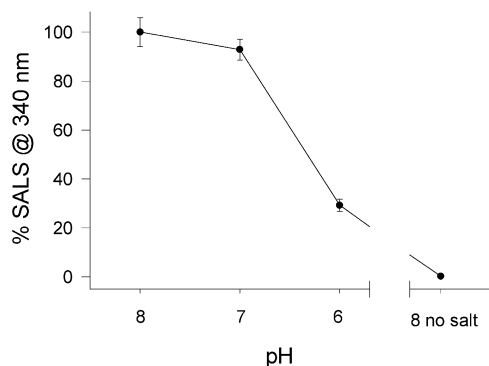


Fig. 3. Extent of core formation as determined by single angle light scatter (SALS). The effect of pH and ionic strength on in vitro assembly of N His6-CA (60 μ M) was measured by single angle light scatter at 340 nm and 90° scattering angle. The dots represent the average of six trials and the error bars are the standard deviations. At pH 8 no salt, the error bar is within the symbol.

a function of pH. Starting at an initial value of pH 8.0 (Fig. 3), we find that lowering the pH decreases the average scattering value to 93% at pH 7 and 29% at pH 6. These results correlate well with the images in Figs. 1 and 2 showing that at pH 8 these proteins assemble in solution and that this assembly can be monitored by light scattering.

The above studies were done at high ionic strength (1 M NaCl). To determine the importance of ionic strength to the assembly process, we started with the assembled protein at pH 8, 1 M NaCl and removed the salt from the buffer solution by dialysis. Using light scattering (Fig. 3), we find complete disruption (i.e. from a normalized value of 100% to 3%) of cores showing that the presence of ions is necessary for assembly to occur. This same low value was seen in a protein concentration range of 2–67 μ M (data not shown).

To better understand the basis for the pH-induced oligomerization, we conducted dynamic angle light scattering of the dissociated protein at low ionic strength. We measured the change in hydrodynamic radius, assuming a spherical protein, of the immature capsid solution at 20 μ M protein and without salt. We find a reduction in radius from 3.74 to 3.52 nm as the pH is raised from 6.0 to 8.0 (Fig. 4). These results indicate a condensation of the protein with increasing pH.

3.2. Binding of cyclophilin A to N His6-CA is dependent on capsid's potential to form cores

The data presented above show that we can monitor the assembly of immature capsid in solution by light scattering. This ability allows us to test factors that may play either a direct or indirect role in assembly. One of these factors is CypA. At some point before the release of the immature virus from infected host cells, the cellular protein cyclophilin A binds to the capsid domain of Gag and becomes incorporated into HIV-1 virions [8–10]. Since cyclophilin A binds to Pro90 of capsid [12,13] in the immature state, it is possible that the *cis-trans* proline isomerase activity of CypA is important in promoting maturation of the capsid domain of Gag.

Using fluorescence spectroscopy, we first quantified the interaction energy between CypA and N His6-CA. To carry out these measurements, CypA was titrated into acrylodan-labeled N His6-CA in 100 mM NaH_2PO_4 at pH 6, 7 and 8, the resulting data were fitted to a bimolecular dissociation constant (see Section 2). We found that the apparent dissociation constant for cyclophilin A binding to acrylodan-labeled N His6-CA at pH 7.0 was similar to that found at pH 8.0 (13 ± 6 nM and 31 ± 3 nM, respectively; Fig. 5). We confirmed

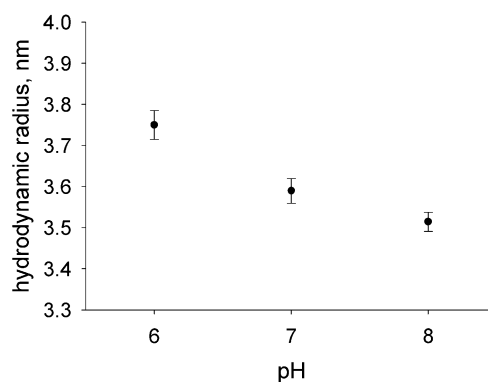


Fig. 4. The effect of pH on N His6-CA as measured by dynamic angle light scattering. N His6-CA (20 μ M) in 100 mM NaH_2PO_4 was centrifuged at $16\,000 \times g$ for 20 min. The gray open circles represent an individual trial, the black closed circles represent the mean of the trials and the error bars are the standard deviations.

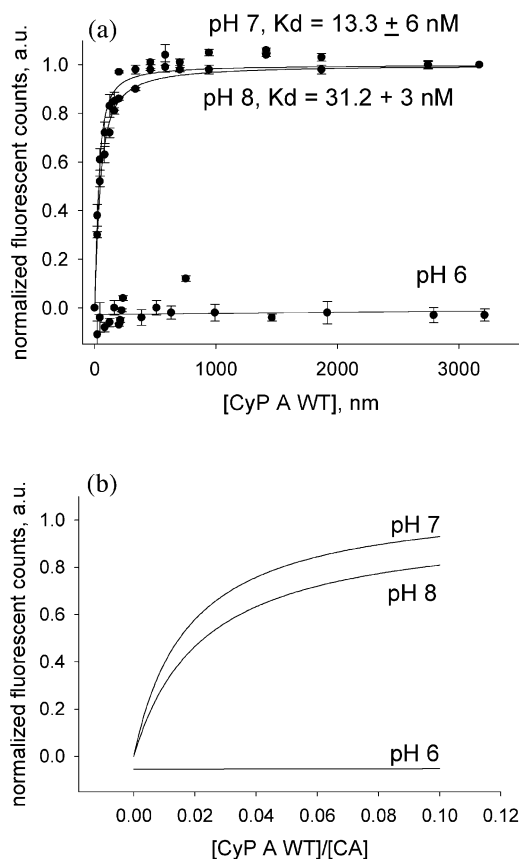


Fig. 5. The effect of pH on cyclophilin A binding to N His6-CA was measured by fluorescence spectroscopy. Panel (a) shows binding under stoichiometric conditions while Panel (b) shows binding under physiological conditions. The dots represent the average of three trials and the error bars are the standard deviations. CypA is cyclophilin A and CA is N His6-CA.

that the change in acrylodan-labeled N His6-CA with increasing amounts of CypA reflected a protein–protein interaction by repeating the titrating at pH 7.0 at different initial values of acrylodan-labeled N His6-CA, and showing that the resulting K_d is unchanged within error (data not shown).

The physiological stoichiometry of CypA to CA has been found to be 1:10 [8,11,38], but it is unclear whether this protein ratio is due to the intrinsic thermodynamic binding behavior of the proteins, or whether the stoichiometry is altered by the local availability of CypA and/or the

occlusion of binding sites in the oligomerizing Gag. In the inset in Fig. 5, we show an expanded version of the beginning of the titration curve. We find that at pH 7.0 and pH 8.0 saturation is reached at 1:10 CypA/capsid, even though all potential CypA binding sites on the capsid should be available under these conditions. Thus, the conformation of the immature form of the capsid is responsible for recruiting CypA into the virion at a specific conformation.

Interestingly, at pH 6.0 we could not detect association between acrylodan-labeled N His6-CA and CypA. Thus, this more extended immature capsid structure can neither oligomerize nor bind CypA.

3.3. Cyclophilin A does not affect the rate of N His6-CA oligomerization

The preference of cyclophilin A for the ‘oligomerization-ready’ form of N His6-CA suggests that CypA may promote oligomerization by stabilizing this form of the protein. To test this possibility, we measured the rate of N His6-CA oligomerization by monitoring single angle light scatter of the protein at 67 μ M in the presence and absence of cyclophilin A (6 μ M) as a function of time. The raw data are shown in Fig. 6. We find that the presence of cyclophilin A does not affect the initial rate of capsid oligomerization.

3.4. Cyclophilin A does not affect the stability of N His6-CA cores

Since CypA did not affect the rate of core formation, it is possible that its presence in the immature cores may alter the stability of the immature capsid–capsid protein contacts through its *cis-trans* isomerase activity. We tested this idea using high hydrostatic pressure. The application of high hydrostatic pressure to a protein complex will cause dissociation due to the decrease in volume achieved as solvent is forced into the cavities left by inefficient protein packing at the subunit interfaces. In general, the steepness of a pressure–dissociation curve as well as the midpoint is indicative of the energetics and efficiency of the

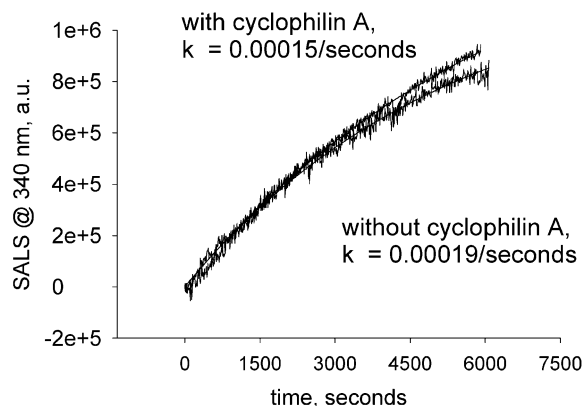


Fig. 6. Initial rate of core formation. N His6-CA (60 μ M) in 50 mM Tris, pH 8 and 1 M NaCl was incubated at 37 $^{\circ}$ C while its oligomerization state was monitored using single angle light scatter (SALS) with an incident light of 340 nm set at a 90 $^{\circ}$ scattering angle. This was repeated in the presence of cyclophilin A (6 μ M) at the physiologically relevant ratio of 1 cyclophilin A molecule for every 10 capsid molecules. The ordinate is measured in arbitrary units (a.u.).

subunit interfaces and in turn, the strength of the association.

We first formed the N His6-CA cores in the presence of CypA (1:10) by raising the pH to 8.0 and increasing the ionic strength by the addition of 1 M NaCl. We monitored the aggregation state of the N His6-CA cores by single angle light scattering as a function of hydrostatic pressure. The application of pressure up to 2000 bars caused complete dissociation of the aggregates as compared to values obtained from control curves made at atmospheric pressure. In Fig. 7 we find that the pressure dissociation curve was unchanged in the presence of CypA indicating that CypA does not affect the stability of immature capsid cores

4. Discussion

In this study, we have shown that the formation of spherical immature-like cores of capsid requires at least two conditions, a neutral or slightly basic pH and a relatively high ionic strength. This observation allowed us to test the conditions in which the host protein, CypA is recruited into the virion and the repercussions of this recruitment on the assembly processes.

We begin this study by verifying that our model of immature capsid, N His6-CA is appropriate. We did this by viewing the aggregation of the protein by electron and atomic force microscopy as well as single angle light scattering. The observation that this construct would form spherical particles or cores was expected based on previous structural studies showing that removal of the N-terminus of capsid is an absolute requirement to induce the transition from the spherical, immature structures to the conical mature capsid [25–27].

Our data show a strong pH dependence of immature capsid assembly. The mature capsid has an isoelectric point of 6.7 and we previously found that at high ionic strengths, decreasing the pH from 8 to 6 results in dissociation of capsid aggregate to monomers [34]. Here, we found that our immature capsid formed cores more efficiently at pH 8 and 7 as opposed to pH 6, as predicted from previous electron microscopy studies [26]. The observation that oligomerization of both mature and immature capsid is inhibited below pH 7 indicates that protonation of some population of residues in the capsid–capsid association region is responsible. The single His residue, His226, in the

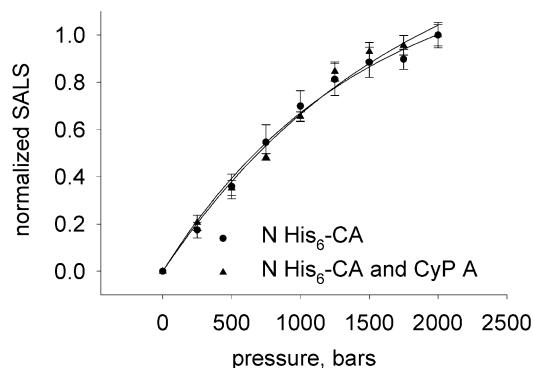


Fig. 7. Stability of cores. N His6-CA (60 μ M) in 50 mM Tris pH 8 and 1 M NaCl was incubated at 37 $^{\circ}$ C for 1 h. The aggregates were pressurized and their oligomerization state was monitored using single angle light scatter (SALS) with an incident light of 340 nm set at a 90 $^{\circ}$ scattering angle. This was repeated in the presence of cyclophilin A (CypA, 6 μ M) at the physiologically relevant ratio of 1 cyclophilin A for every 10 capsid molecules. The data points represent the average of five experiments. The error bars represent standard deviations. The ordinate is measured in arbitrary units (a.u.).

domain responsible for oligomerization (i.e. the C-terminal domain), is a candidate. We can speculate that since capsid in virions is subject to a highly electronegative environment due to anionic lipid head groups and RNA, the pH dependence of oligomerization may stabilize the aggregated form.

We have also found that oligomerization of immature capsid is solely dependent on ionic strength because, in the absence of salt, N His6-CA was unable to form cores even at pH 8. Our dynamic light scattering studies show that at pH 8, the immature capsid is more condensed. Thus, the combination of deprotonating critical groups and shielding the charge of others is necessary for the subunits to self-associate. We stress that we could not find evidence of large scale protein unfolding at pH 6 as shown here, by a small increase (0.22 nm) in hydrodynamicity by dynamic light scattering.

Our studies also show a strong pH dependence of CypA binding to immature capsid. Presently, the requirement of CypA for efficient infectivity of HIV-1 is unknown [39]. It is known that CypA is incorporated into HIV-1 virions by specific interaction with Pro90 of capsid at a 1:10 CypA/CA ratio [8,10,11,38] and since cyclophilin A is a *cis-trans* proline isomerase, it is possible that it mediates the conformational changes in the capsid domain of Gag needed for proper assembly.

Tight binding affinities for CypA were measured for pH 8 and 7, while binding at pH 6 was too weak to be quantified. These dissociation constants are three orders of magnitude higher than the previously reported value of 16 ± 4 μ M obtained for CypA binding to full length mature form capsid [15] implying that CypA has a higher affinity for capsid in the context of Gag. This hypothesis is supported by experiments using ELISA (enzyme-linked immunosorbent assay) which quantitatively showed that cyclophilin bound tighter to capsid when recombinants contained at least 12 carboxy terminal amino acids from matrix in addition to capsid then when recombinants contained only capsid [40]. We could not detect CypA association to N His6-CA at pH 6, which is most likely due to protonation of His87 in the CypA binding site. Alternately, the lack of CypA binding at pH 6 may

result from large scale conformational changes in either of the two proteins.

Under conditions where all CypA binding sites on immature CA should be available, the stoichiometry of the complexes is identical to that seen in the virion. This finding argues against the idea that factors limiting 1:1 stoichiometry (e.g. protein availability, occlusion of binding sites, etc.) exist during assembly and argue that stoichiometry is dictated by the isomeric form of Pro90 in the CypA binding pocket.

We tested the idea that CypA may play a role in promoting the formation of cores possibly through its proline *cis-trans* isomerase activity by measuring the rate of N His6-CA oligomerization in the presence and absence of CypA. Both samples showed identical rates in the first hour of assembly. Minor differences in rates at longer times where cores had formed prompted us to test whether CypA alters the stability of the cores. High-pressure dissociation studies showed no difference in the dissociation of cores formed in the presence or absence of CypA. Thus, core stability is due to the protein–protein contacts between the capsid subunits themselves without involvement of CypA or the CypA binding site on capsid. Taken together, our data thus suggest that CypA may not play a role in assembly, but the cyclophilin A/capsid interaction instead serves as entry point into the HIV-1 virion. The role of CypA in disassembly of mature capsid is now being tested.

Acknowledgments

We greatly acknowledge the help of Dr El-Maghrabi in the design of the constructs, Margaret Luk-Paszyc for help with the dynamic light scattering measurements, and Paxton Provitera, Louisa Dowal, Finally, Philip and Drs Yianjian Guo and Naraynan for helpful discussions. This work was supported by NIH GM58271 and the Turner Foundation.

References

- [1] J.M. Coffin, S.H. Hughes, H.E. Varmus, *Retroviruses*, Cold Spring Harbor Laboratory Press, Inc, Plainview, NY, 1997.

- [2] M.I. Bukrinsky, S. Haggerty, M.P. Dempsey, N. Sharova, A. Adzhubei, L. Spitz, et al., *Nature* 365 (1993) 666–669.
- [3] U. von Schwedler, K.S. Kornbluth, D. Trono, *Proc. Natl. Acad. Sci. USA* 91 (1994) 6992–6996.
- [4] N. Heinzinger, M. Bukinsky, S. Haggerty, A. Ragland, V. Kewalrammi, M.-A. Lee, et al., *Proc. Natl. Acad. Sci. USA* 91 (1994) 7311–7315.
- [5] D. Braaten, E. Franke, J. Luban, *J. Virol.* 70 (1996) 3551–3560.
- [6] G. Fischer, B. Wittmann-Liebold, K. Lang, T. Kiefhaber, F.X. Schmid, *Nature* 337 (1989) 476–478.
- [7] E.K. Baker, N.J. Colley, C.S. Zuker, *Embo. J.* 13 (1994) 4886–4895.
- [8] E.K. Franke, H.E. Yuan, J. Luban, *Nature* 372 (1994) 359–362.
- [9] M. Thali, A. Bukovsky, E. Kondo, B. Rosenwirth, C.T. Walsh, J. Sodroski, et al., *Nature* 372 (1994) 363–365.
- [10] J. Luban, K.L. Bossolt, E.K. Franke, G.V. Kalpana, S.P. Goff, *Cell* 73 (1993) 1067–1078.
- [11] D.E. Ott, L.V. Coren, D.G. Johnson, R.C. Sowder II, L.O. Arthur, L.E. Henderson, *AIDS. Res. Hum. Retroviruses* 11 (1995) 1003–1006.
- [12] M. Schutkowski, M. Drewello, S. Wollner, M. Jakob, U. Reimer, G. Scherer, et al., *FEBS. Lett.* 394 (1996) 289–294.
- [13] T.R. Gamble, F.F. Vajdos, S. Yoo, D.K. Worthylake, M. Houseweart, W.I. Sundquist, et al., *Cell* 87 (1996) 1285–1294.
- [14] F.F. Vajdos, S. Yoo, M. Houseweart, W.I. Sundquist, C.P. Hill, *Protein Sci.* 6 (1997) 2297–2307.
- [15] S. Yoo, D.G. Myszk, C. Yeh, M. McMurray, C.P. Hill, W.I. Sundquist, *J. Mol. Biol.* 269 (1997) 780–795.
- [16] J. Colgan, H.E. Yuan, E.K. Franke, J. Luban, *J. Virol.* 70 (1996) 4299–4310.
- [17] E. Mlynar, D. Bevec, A. Billich, B. Rosenwirth, A. Steinkasserer, *J. Gen. Virol.* 78 (4) (1997) 825–835.
- [18] A. Steinkasserer, R. Harrison, A. Billich, F. Hammerschmid, G. Werner, B. Wolff, et al., *J. Virol.* 69 (1995) 814–824.
- [19] D. Braaten, H. Ansari, J. Luban, *J. Virol.* 71 (1997) 2107–2113.
- [20] T. Dorfman, A. Weimann, A. Borsetti, C.T. Walsh, H.G. Gottlinger, *J. Virol.* 71 (1997) 7110–7113.
- [21] D. Braaten, E.K. Franke, J. Luban, *J. Virol.* 70 (1996) 3551–3560.
- [22] B. Ackerson, O. Rey, J. Canon, P. Krogstad, *J. Virol.* 72 (1998) 303–308.
- [23] D. Braaten, J. Luban, *Embo. J.* 20 (2001) 1300–1309.
- [24] L.B. Kong, D. An, B. Ackerson, J. Canon, O. Rey, I.S. Chen, et al., *J. Virol.* 72 (1998) 4403–4407.
- [25] C. Tang, Y. Ndassa, M.F. Summers, *Nat. Struct. Biol.* 9 (2002) 537–543.
- [26] I. Gross, H. Hohenberg, C. Huckhagel, H.G. Krausslich, *J. Virol.* 72 (1998) 4798–4810.
- [27] U.K. von Schwedler, T.L. Stemmler, V.Y. Klishko, S. Li, K.H. Albertine, D.R. Davis, et al., *EMBO J.* 17 (1998) 1555–1568.
- [28] L.S. Ehrlich, B.E. Agresta, C.A. Carter, *J. Virol.* 66 (1992) 4874–4883.
- [29] I. Gross, H. Hohenberg, H.G. Krausslich, *Eur. J. Biochem.* 249 (1997) 592–600.
- [30] E. Schmalzbauer, B. Strack, J. Dannull, S. Guehmann, K. Moelling, *J. Virol.* 70 (1996) 771–777.
- [31] R.D. Berkowitz, J. Luban, S.P. Goff, *J. Virol.* 67 (1993) 7190–7200.
- [32] P. Provitera, A. Goff, A. Harenberg, F. Bouamr, C. Carter, S. Scarlata, *Biochem.* 40 (2001) 5565–5572.
- [33] L. Ratner, W. Haseltine, R. Patarca, K.J. Livak, B. Starcich, S.F. Josephs, et al., *Nature* 313 (1985) 277–284.
- [34] L.S. Ehrlich, T. Liu, S. Scarlata, B. Chu, C.A. Carter, *Biophys. J.* 81 (2001) 586–594.
- [35] I. Gross, H. Hohenberg, C. Huckhagel, H.-G. Krausslich, *J. Virol.* 72 (1998) 4798–4810.
- [36] U. Von Schwedler, T. Stemmler, V. Klishko, S. Li, K. Albertine, D. Davis, et al., *EMBO J.* 17 (1998) 1555–1568.
- [37] C. Berthet-Colominas, S. Monaco, A. Novelli, G. Sibai, F. Mallet, S. Cusack, *EMBO J.* 18 (1999) 1124–1136.
- [38] M. Thali, A. Bukovsky, E. Kondo, B. Rosenwirth, C. Walsh, J. Sodroski, et al., *Nature* 372 (1994) 363–365.
- [39] A.A. Bukovsky, A. Weimann, M.A. Accola, H.G. Gottlinger, *Proc. Natl. Acad. Sci. USA* 94 (1997) 10943–10948.
- [40] R. Bristow, J. Byrne, J. Squirell, H. Trencher, T. Carter, B. Rodgers, et al., *J. Acquired Immune Defic. Syndr. Hum. Retrovirol.* 20 (1999) 334–336.